7-1-2006

Consequences of disk scale height on lisa confusion noise from close white dwarf binaries

M. Benacquista

K. Holley-Bockelmann

Recommended Citation

M. Benacquista, et. al., (2006) Consequences of disk scale height on lisa confusion noise from close white dwarf binaries.Astrophysical Journal645:1 I589. DOI: http://doi.org/10.1086/504024

The Astrophysical Journal, 645:589–596, 2006 July 1

CONSEQUENCES OF DISK SCALE HEIGHT ON *LISA* CONFUSION NOISE FROM CLOSE WHITE DWARF BINARIES

M. Benacquista
Department of Sciences, Montana State University–Billings, Billings, MT 59101

and

K. Holley-Bockelmann
Department of Astronomy and the Center for Gravitational Wave Physics, Pennsylvania State University, University Park, PA 16802
Received 2005 April 5; accepted 2006 March 7

ABSTRACT

Gravitational radiation from the Galactic population of close white dwarf binaries (CWDBs) is expected to produce a confusion-limited signal at the lower end of the sensitivity band of the *Laser Interferometer Space Antenna* (*LISA*). The canonical scale height of the disk population has been taken to be 90 pc for most studies of the nature of this confusion-limited signal. This estimate is probably too low, and the consequences of a more realistic scale height are investigated with a model of the *LISA* signal due to populations of CWDBs with different scale heights. If the local space density of CWDBs is held constant, increasing the scale height results in both an increase in the overall strength of the confusion-limited signal as well as an increase in the frequency at which the signals become individually resolvable. If the total number of binaries is held constant, increasing the scale height results in a reduction of the number of expected bright signals above the confusion-limited signal at low frequencies. We introduce an estimator for comparing this transition frequency that takes into account the signal spreading at higher frequencies.

Subject headings: binaries: close — Galaxy: structure — gravitational waves — white dwarfs

1. INTRODUCTION

The *Laser Interferometer Space Antenna* (*LISA*) is a planned space-based gravitational radiation detector that will have a sensitivity band in the range of 10^{-5} to 10^{-1} Hz. Many of the target sources for *LISA* will be supermassive and intermediate mass black hole inspirals, as well as extreme mass ratio inspirals of stellar mass compact objects into these more massive black holes. At the lower end of the sensitivity band, the primary noise source will not be instrumental but rather will come from the accumulated signal of millions of close white dwarf binaries (CWDBs) in the Galaxy. If we interpret the signal as many overlapping sources, this signal is expected to dominate the instrumental noise above $\sim$0.2 mHz. At higher frequencies, the signal will start to separate into individually resolvable sources as the number density of ultracompact binaries falls with increasing frequency. In most studies of the sensitivity and science capabilities of *LISA*, this confusion-limited signal is modeled as an additional Gaussian and stationary noise source in the frequency range between 0.1 and 3 mHz (e.g., Cutler 1998; Barack & Cutler 2004a, 2004b).

The overall shape and placement of the confusion-limited noise source is usually based on the original work of Hils et al. (1990), who calculated the expected signal from a number of different binary systems in the Milky Way. The expected signal due to CWDBs was shown to dominate all other Galactic sources between 0.1 and 3 mHz. Their calculation of the expected population of CWDBs was ostensibly based on a surface density star formation rate, which is independent of the scale height of any Galactic spatial distribution model. However, they then compared the local space density of their model with observations and concluded that a factor of 10 reduction of the total number of binaries would bring their model more in line with observations. This amounts to a de facto calibration of the total number of binaries by local space density. The calculation of the local space density is dependent on their Galactic spatial distribution model

$$\rho(\boldsymbol{r}) = \frac{N}{4\pi R_0^2 z_0} e^{-R/R_0} e^{-|z|/z} \tag{1}$$

(Hils et al. 1990), which is a double exponential with a radial scale $R_0 = 3.5$ kpc and a disk scale height $z = 90$ pc. The choice of $z_0 = 90$ pc follows from the fact that the mass of the CWDB progenitors are relatively massive, lying in a critical range between 1.12 and 5.6 $M_\odot$ (Webbink 1984). It is this reduced population that is used to generate the white dwarf binary background in the *LISA* sensitivity curve generator.[1]

More recent simulations of the Galactic white dwarf binary population have used a number of different spatial distributions (Edlund et al. 2005; Nelemans 2003; Nelemans et al. 2001a). The most recent simulation of Edlund et al. (2005) used the probability distribution

$$\mathcal{P}(R,\ z) = \frac{1}{4\pi R_0^2 z_0} e^{-R/R_0} \mathrm{sech}^2(z/z_0), \tag{2}$$

where R_0 and z_0 are the radial scale and scale height, respectively. Others have included a bulge by effectively doubling the star formation rate in the inner regions of the Galaxy and adding a bulge density of

$$\rho_{\mathrm{bulge}} \propto e^{-[r/(0.5\ \mathrm{kpc})]^2} \tag{3}$$

(Nelemans 2003), where $r = (x^2 + y^2 + z^2)^{1/2}$ in kpc. The Galactic white dwarf model used to generate the confusion noise of Barack & Cutler (2004a, 2004b) is based on the population

[1] See http://www.srl.caltech.edu/~shane/sensitivity/MakeCurve.html.

synthesis of Nelemans et al. (2001a). Through an error in the radial probability distribution function, the spatial distribution actually used was of the form

$$\rho(\boldsymbol{r}) = \frac{N}{4\pi R R_0 z_0} e^{-R/R_0} \mathrm{sech}^2(z/z_0), \tag{4}$$

which unintentionally does a reasonable job of simulating a bulge (Nelemans 2003). In all three cases above, the radial scale was $R_0 = 2.5$ kpc, and the scale height was $z_0 = 200$ pc.

It is a well-known fact that different classes of stars have different scale heights (Gilmore & Reid 1983; Kuijken & Gilmore 1989; Kent et al. 1991; Marsakov & Shevelev 1995; Ojha et al. 1996; Reed 2000; Siebert et al. 2003), and that for main-sequence stars, the more massive ones live in thinner disks (e.g., Miller & Scalo 1979). While it is true that the current crop of high-mass main-sequence stars are found in a thin disk, CWDBs are evolved systems, many of which are much older than the $\mathcal{O}(10^7)$ yr implied by the main-sequence lifetimes of the most massive CWDB progenitors. Any evolved population is known to exhibit a large scale height that is proportional to its vertical velocity dispersion (Nelson et al. 2002; Mihalas & Binney 1981; Wielen 1977; Allen 1973, 247). There is some debate as to *why* old stellar populations live in thicker disks. Perhaps the thickness is simply an artifact of the conditions of the primordial galaxy, when stars were formed from gas clumps within a galaxy potential that was still collapsing to form the disk (Eggen et al. 1962) or were easily scattered by an environment rich in galaxy mergers (Steinmetz & Navarro 2002). On the other hand, interactions with potential fluctuations from molecular clouds and other small-scale perturbations may heat an initially cold stellar population, creating an ever thicker disk as it ages and experiences more encounters (Schröder & Pagel 2003).

Whatever the reason, it is clear that the vertical scale height for white dwarfs is rather thick—current estimates place z_0 between 240 and 500 pc (Nelson et al. 2002). In light of these estimates, we have chosen scale heights of 90 and 500 pc to investigate the consequences of a larger scale height on the nature of the expected gravitational wave signal from CWDBs in the Galaxy. To minimize the effect of using different population synthesis models, we compare these two scale heights using our own population model. We anticipate similar behavior if one were to change the scale height of a different population model. In order to compare the resulting gravitational wave signals, we introduce a tool for characterizing the separation of strong signals in the frequency domain.

2. POPULATION MODEL

The population model we use to generate the different populations of the CWDBs is modified slightly from the population model described in Benacquista et al. (2004). In this model, the binary types at birth are assigned a probability based on the population synthesis of Nelemans et al. (2001b), assigned an age based on an assumed constant birth rate, and then placed in the galaxy based on probability distributions in cylindrical coordinates R and z given by

$$P(R)\,dR = \frac{R\,dR}{R_0^2} e^{-R/R_0}, \tag{5}$$

$$P(z)\,dz = \frac{dz}{2z_0} \mathrm{sech}^2(z/z_0), \tag{6}$$

where R_0 is the radial scale length and z_0 is the scale height. In order to investigate the effects of different scale heights, we have chosen to keep a fixed value of radial scale $R_0 = 2500$ pc and have varied only the scale height and the total number of binaries. The space density of binaries, $\rho(\boldsymbol{r})$, is found from the total number, N, and the probability distributions by

$$\rho(\boldsymbol{r}) = N\mathcal{P}(R,\ z), \tag{7}$$

where $\mathcal{P}$ is given by equation (2). We assume that the solar neighborhood is located at $R_e = 8500$ pc and $z_e = 0$ pc and define the local space density to be $\rho_e = \rho(R_e,\ z_e)$. We then obtain $\rho_e = (4.25 \times 10^{-10}\ \mathrm{pc}^{-2})N/z_0$ for the local space density. For our baseline thin-disk model (Thin model), we choose $z_0 = 90$ pc and $N = 3 \times 10^6$, so that $\rho_e = 1.4 \times 10^{-5}\ \mathrm{pc}^{-3}$. We have chosen this value to most closely mimic the reduced population used by Hils et al. (1990). To obtain the same local space density using the distribution of equation (4) (Nelemans et al. 2001a), one would need to take $N = 2.2 \times 10^7$ (1.0×10^7) for a scale height of 200 pc (90 pc). Assuming that roughly 10% of white dwarfs are in binary systems and about 10% of these are CWDBs with orbital period less than 2×10^4 s, this is about a factor of 3 below a conservative estimate of the expected local white dwarf space density of $4 \times 10^{-3}\ \mathrm{pc}^{-3}$ (Knox et al. 1999). For our larger scale height model (Thick A model), we choose $z_0 = 500$ pc and $N = 1.67 \times 10^7$. This model has the same local space density as our baseline model. To investigate the effect of the increased total number in the Thick A model, we have also introduced a model with the same total number as the Thin model, $N = 3 \times 10^6$ but a scale height of $z_0 = 500$ pc (Thick B model). These three models are summarized in Table 1.

TABLE 1
Disk Population Model Parameters

Model	z_0 (pc)	N (10^6)	ρ_e (10^{-6} pc^{-3})
Thin	90	3	14
Thick A	500	16.7	14
Thick B	500	3	2.6

We have used the Michelson signal as the observable for the expected *LISA* data stream. The data stream is calculated in the long wavelength approximation for binaries whose central gravitational wave frequency is below 3 mHz (see Rubbo et al. [2004] or Cutler [1998] for descriptions of this approximation). At higher frequencies ($f \gtrsim 3$ mHz), we have used the rigid adiabatic approximation (see Rubbo et al. [2004] or Vecchio & Wickham [2004] for a description of this approximation). We have included a linear chirp for those binaries whose frequency will shift by more than $\sim 3 \times 10^{-9}$ Hz during the 1 yr observation. We have generated three realizations of each of our Galaxy models. To minimize any variations between models, we used the same three initial random seeds to generate the three realizations of each model. Thus, the first realization of the Thin model has exactly the same population of binaries as the first realization of the Thick B model (modulo a rescaling of the z-coordinate), and the first realization of the Thick B model is a subset of the first realization of the Thick A model. Representative strain spectral densities for the three models are shown in Figures 1–3. To better characterize the spectra, we have also included a running median over 1000 bins for each spectrum. For reference, we have also included the *LISA* sensitivity curve (at S/N = 1) and the standard Hils-Bender CWDB confusion curve as generated by the *LISA* sensitivity curve generator. Because our spectra are calculated in the detector frame and the

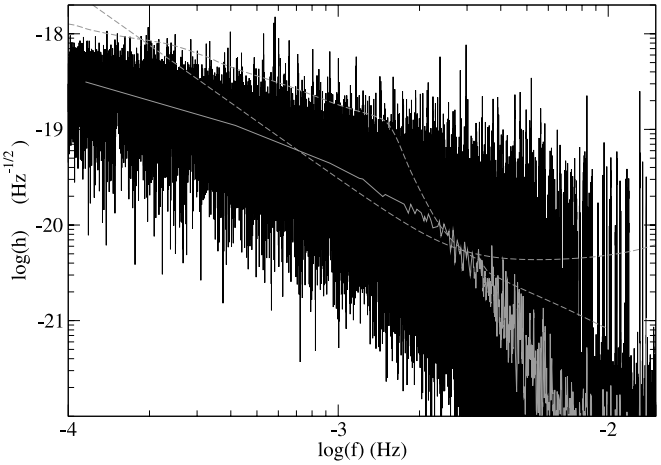

FIG. 1.—Strain spectral density (*black*) for the Thin model with a running median over 1000 bins (*gray*). The expected noise level and standard Hils & Bender (1997) confusion-limited noise from the *LISA* sensitivity curve generator are shown as the light gray dashed curves. The noise and standard confusion-limited noise curves have been multiplied by $(3/20)^{1/2}$ to transform them from the barycenter frame to the detector frame.

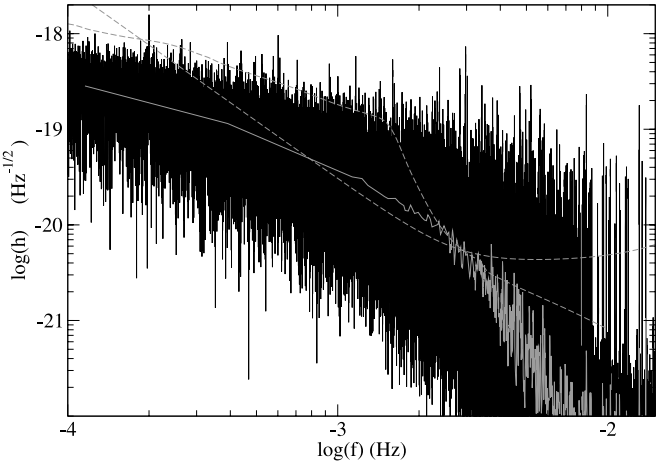

FIG. 3.—Strain spectral density (*black*) for the Thick B model with a running median over 1000 bins (*gray*). The expected noise level and standard Hils & Bender (1997) confusion-limited noise from the *LISA* sensitivity curve generator are shown as the light gray dashed curves. The noise and standard confusion-limited noise curves have been multiplied by $(3/20)^{1/2}$ to transform them from the barycenter frame to the detector frame.

sensitivity curve generator output is in the barycenter frame, we have rescaled the sensitivity curve generator output by $(3/20)^{1/2}$ to account for averaging over all polarizations and directions.

The strain spectra for the models show the expected behavior—there is a foreground of strong nearby signals superimposed on a confusion-limited background at frequencies below about 1 mHz, numerous individually resolvable signals above about 10 mHz, and a transition zone in between where the floor of the strain spectral density drops to the numerical noise level of $\sim 10^{-22}$ Hz$^{-1/2}$. We note that the running median of our spectra is generally below the standard Hils-Bender curve. This is due to the fact that we are using a population synthesis based on the binary evolution of Nelemans et al. (2001b), and this tends to produce binaries whose chirp mass is roughly a factor of 2 lower than the population synthesis of Hils et al. (1990; G. Nelemans 2005, private communication). However, if one scales up the running median curve so that it coincides with the standard Hils-Bender curve, one notices that for each model there is still considerable signal noise beyond the standard upper confusion limit of 3 mHz, and that the noise level drops much more slowly than the standard confusion curve. This is shown in Figure 4 for the Thin model, which best matches the Hils et al. (1990) CWDB population. We caution, however, that it is misleading to quantitatively compare the specific characteristics of the standard CWDB curve to the Thin model—the population synthesis model is different, the approach to data analysis is different, and we define a different measure of the confusion onset (see § 3). Consequently, the standard confusion curve on these figures should be used merely as a qualitative benchmark.

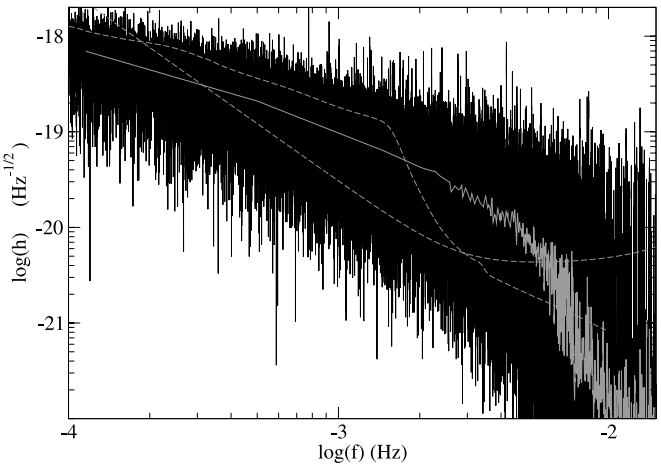

FIG. 2.—Strain spectral density (*black*) for the Thick A model with a running median over 1000 bins (*gray*). The expected noise level and standard Hils & Bender (1997) confusion-limited noise from the *LISA* Sensitivity Curve Generator are shown as the light gray dashed curves. The noise and standard confusion-limited noise curves have been multiplied by $(3/20)^{1/2}$ to transform them from the barycenter frame to the detector frame.

3. ESTIMATING THE TRANSITION FREQUENCY

Characterizing the shape and amplitude of the unresolvable gravitational wave sources is not a trivial undertaking, and many groups are working to develop techniques to extract both the resolvable signals from the confusion foreground (cf. Umstätter et al. 2005a, 2005b; Cornish & Larson 2003a, 2003b; Takahashi

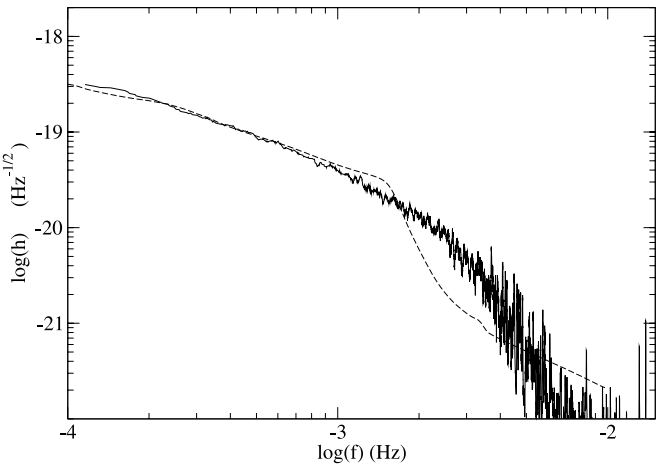

FIG. 4.—Running median of the Thin model over 1000 frequency bins compared with the standard CWDB confusion curve from the *LISA* sensitivity curve generator scaled to coincide with the Thin model at low frequencies.

& Seto 2002; Cutler 1998) and to quantify the extent of the foreground itself (Hils et al. 1990; Nelemans et al. 2001a; Bender & Hils 1997; Evans et al. 1987; Postnov & Prokhorov 1998; Timpano et al. 2006). Since these techniques are still in development, there is no canonical and robust way to quantify the onset of the confusion limit. We develop and present one statistic in this section; however, we caution that we are using it primarily as a comparison tool to discover trends *among our models*, and it should not be used to compare our results with those of other published work. For a given data analysis technique, however, the same trends should be obtained.

The conversion of the raw Galactic spectrum to a smooth curve representing the confusion limit is subject to a number of assumptions concerning both the ability to remove stronger foreground signals from the low-frequency region and to individually resolve and extract signals from the higher frequency regions where there are both full and empty frequency bins. Depending on how optimistically one chooses to estimate these abilities, one can dramatically alter the shape of the Galactic confusion curve. For example, the method described in Hils & Bender (1997) assumes that information in three frequency bins are required to completely parameterize (and therefore subtract) the signal from an individual binary. These three bins are removed at the signal strength of the foreground binary. The effect of this assumption is to produce the dramatic drop in the standard white dwarf binary curve at around 3 mHz where the average number of binaries per frequency bin drops below 1. Timpano et al. (2006) have used a different method to estimate the ability to remove signals in the transition zone. Starting with the full signal from the entire population of binaries, they calculate a running median to determine the background level of the full signal. Next, they determine the bright binaries that stand above this level with a S/N of at least 5. These binaries are then completely and exactly removed from the data stream. The process is then repeated on the remaining signal until the number of new bright binaries is less than 1% of the previously found bright binaries, resulting in a remaining signal that is nearly Gaussian. This process is highly optimistic and therefore represents a lower bound on the cleaned signal. Nelemans et al. (2001a, 2004) simply cut the signal off once the average number of binaries per bin drops below 1. Since these assumptions rely on the currently undemonstrated capabilities of future data analysis techniques, we choose to analyze the signal prior to any assumed data reduction.

3.1. *The ζ Estimator*

Although individual binaries will occupy a single frequency bin in the barycenter frame (unless they are chirping), the motion of *LISA* will spread these signals out over several frequency bins. Consequently, simply counting the number of binaries per bin is not a very realistic way of determining the transition zone. The ability to resolve a signal is related more to the number of adjacent bins without signal than the number of binaries per bin. In order to successfully extract the signal due to a binary, it is necessary to determine parameters (such as sky position, orientation, and amplitude) that fully characterize the spreading of the signal in the frequency domain. The accuracy with which this can be done is related to the signal-to-noise ratio (S/N). Thus, we construct a parameter, ζ, that characterizes the fraction of frequency bins that contain signal with a specified S/N.

To motivate our definition of ζ, we treat the signal strength $h(f)$ in any frequency bin as though it were sampled from a distribution function. In frequency regions where the signal is completely confusion-limited (or pure noise), we take this distribution function to be

$$P(h(f)) = \frac{h(f)}{\sigma_f^2} \exp\left[\frac{-h^2(f)}{2\sigma_f^2}\right], \tag{8}$$

where σ_f is a measure of the averaged signal strength over a suitably small frequency range so that it can be considered constant. From the mean,

$$\langle h\rangle = \int_0^\infty hP(h)\,dh, \tag{9}$$

and the variance,

$$\sigma_h^2 = \int_0^\infty h^2 P(h)\,dh - \langle h\rangle^2, \tag{10}$$

we can construct the dimensionless quantity

$$\zeta = \frac{\sqrt{\sigma_h^2}}{\langle h\rangle} = \sqrt{\frac{4-\pi}{\pi}}. \tag{11}$$

Thus, in the confusion-limited regime, ζ should be well described by equation (11) and should be approximately 0.5.

When the data stream consists of both noise and signal, the signal strength in any frequency bin should then be modeled as if it were sampled from a linear combination of two distribution functions, one for the noise and one for the signals. This function is given by

$$P'(h(f)) = a\frac{h(f)}{\sigma_f^2}\exp\left[\frac{-h^2(f)}{2\sigma_f^2}\right] + (1-a)\frac{h(f)}{(b\sigma_f)^2}\exp\left[\frac{-h^2(f)}{2(b\sigma_f)^2}\right], \tag{12}$$

where a gives the probability that a given frequency bin will be empty (i.e., dominated by instrument noise of strength σ_f) and b is a measure of the signal-to-noise ratio for the average resolvable signal. The value of ζ in this case is given by

$$\zeta = \frac{\left\{4[a+b^2(1-a)] - \pi[a+b(1-a)]^2\right\}^{1/2}}{\sqrt{\pi}[a+b(1-a)]}. \tag{13}$$

When we apply ζ to our simulation of the *LISA* data stream, we compute the mean and variance of the strain spectral density over n frequency bins using

$$\langle h\rangle_i = \frac{1}{n}\sum_{j=i}^{i+n-1} h(f_j), \tag{14}$$

$$\sigma_{\rm hi}^2 = \frac{1}{n}\sum_{j=i}^{i+n-1} h^2(f_j), \tag{15}$$

and construct

$$\zeta_i = \frac{\sqrt{\sigma_{\rm hi}}}{\langle h_i\rangle}. \tag{16}$$

TABLE 2

Transition Frequencies at which ζ Passes through 1.2 for Galaxy Realizations with Different N

N (10^6)	Number of Models	f_t (mHz)
4	3	2.90 ± 0.07
8	6	4.01 ± 0.11
12	1	4.64
20	2	5.56 ± 0.18

In a region of the spectrum where the potentially resolvable sources have S/N given by b, then ζ_i is a measure of the fraction of bins devoid of resolvable signal. Consequently, one can set a threshold value of ζ_i corresponding to the value of a necessary for a given data analysis technique to be able to resolve signals with $\mathrm{S/N} \gtrsim b$.

3.2. *Expected N-Dependence of Transition Frequency*

Without adhering to a specific data analysis technique, the choice for the threshold value of ζ_i is somewhat arbitrary. However, for a given choice of a, we can expect the transition frequency (f_t) at which ζ_i crosses the associated threshold to scale with the total number of binaries (N) according to $f_t \propto N^{3/8}$. In order to understand this scaling, we note that in the expected transition region between 1 and 10 mHz, the number density of binaries in frequency space is governed primarily by the period evolution through gravitational radiation. Therefore, according to Hils et al. (1990),

$$\frac{dN}{df} \propto N f^{-11/3}, \tag{17}$$

TABLE 3

Transition Frequencies for the Disk Population Models

Model	Realization	f_t (mHz)
Thin	1	2.09–2.11
Thin	2	1.79–2.17
Thin	3	1.58–2.20
Thick A	1	2.93–4.42
Thick A	2	3.60–5.03
Thick A	3	3.46–5.35
Thick B	1	2.22
Thick B	2	1.79–2.19
Thick B	3	2.10–2.23

where f is the gravitational wave frequency. At the frequencies of the transition region, the primary source of spreading of the signal into adjacent frequency bins is the Doppler modulation of the signal, so $\Delta f \propto f$. Consequently, at the transition frequency

$$\left|\frac{dN}{df}\right|_{f_t} \propto f_t^{-1} \propto N f_t^{-11/3}, \tag{18}$$

and so we obtain $f_t \propto N^{3/8}$.

In order to test the ability of the ζ estimator to correctly reproduce the expected scaling of f_t with N, we have applied ζ to a broad set of Galaxy realizations using the density distribution given by equation (4) with different values for z_0, R_0, and N. Note that these toy models have a different density distribution than our disk population models, which more closely match Hils et al. (1990); these models serve to test the ζ estimator and

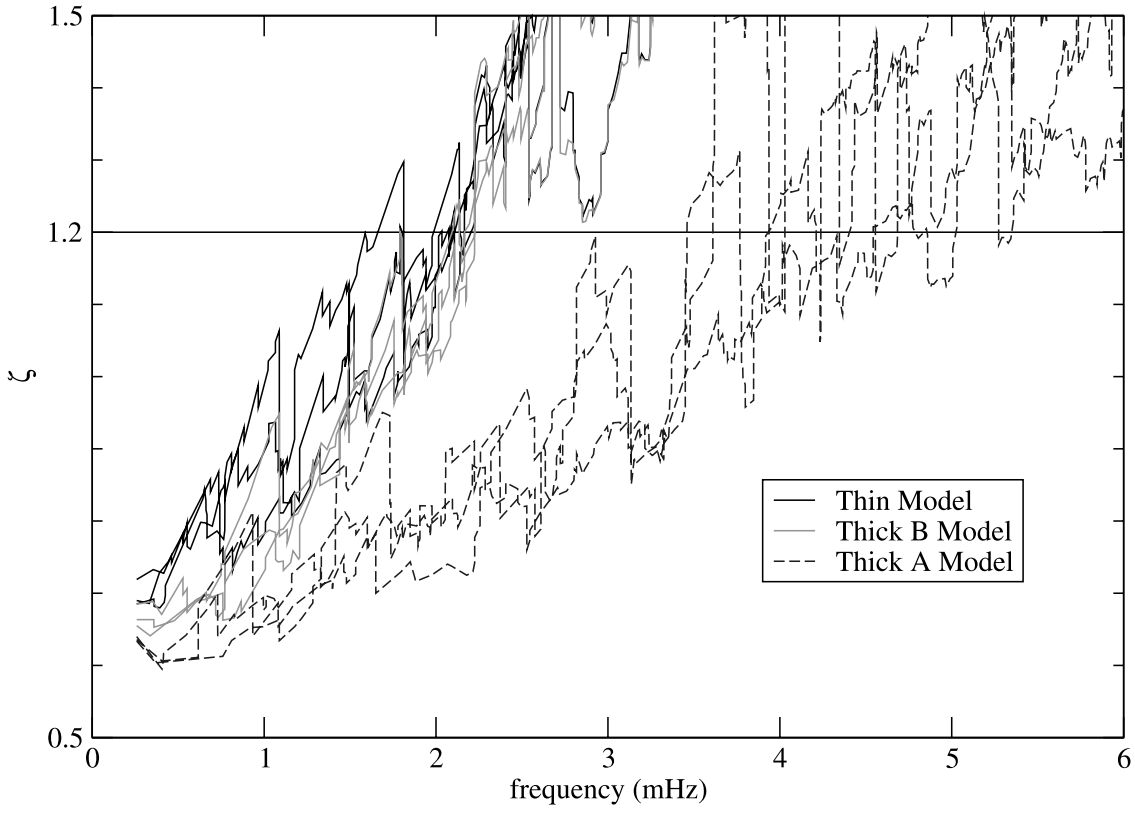

Fig. 5.—ζ for all models in the transition zone. Three realizations are plotted for the Thin (*black line*), Thick A (*dashed dark gray line*), and Thick B (*light gray line*) models.

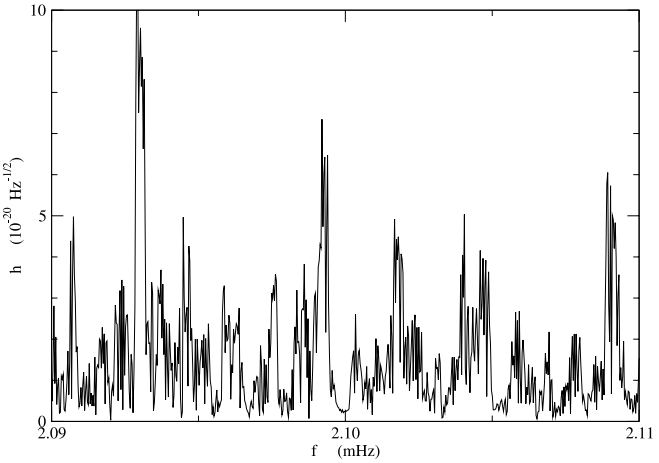

FIG. 6.—Strain spectral density for the Thin model between 2.09 and 2.11 mHz, where ζ passes through 1.2. There are 76 binaries in this region of the spectrum.

determine reasonable values for a, b, and ζ_i. In these realizations, we did not introduce any simulated instrumental noise into the data stream, but numerical round-off errors introduce an effective noise contribution that we estimate from the strain spectral density to be $\simeq 10^{-22}$ Hz$^{-1/2}$. In the expected transition region the mean signal strength, read from the strain spectral density, is $\simeq 10^{-20}$ Hz$^{-1/2}$. Correspondingly, we take $b = 100$ as an approximation of the S/N in the region of interest. We arbitrarily chose $a = 0.5$ to give a threshold value of $\zeta_i = 1.2$. We then chose to average over $n = 20{,}000$ bins to ensure a reasonably smooth curve for ζ. If smaller values of n are used, the effect is to increase the variation in ζ, which increases the spread of frequencies for which ζ passes through the threshold without significantly altering the central value of f_t. The values of f_t obtained in this way are shown in Table 2. A least-squares fit to the values of f_t for a function of the form $f_t = \alpha N^{\beta}$ gives $\beta = 0.39 \pm 0.04$, indicating that ζ does reproduce the correct scaling of the transition frequency with total number.

We note that the ζ estimator is really nothing more than a dimensionless measure of the degree of scatter in the strain amplitude about its mean. It is through the motivation described in equations (8)–(13) that we interpret ζ as a measure of the number of resolvable signals with S/N $> b$. The fact that ζ reproduces the expected scaling of the transition frequency with total number can be viewed as confirmation that this interpretation is reasonable.

4. RESULTS

We have applied the ζ estimator to our model populations to determine the relationship between the transition frequency and the scale height. We calculated the mean and variance as described in equations (14) and (15), averaging over $n = 20{,}000$. Again, as in § 3.2, by inspection of the strain spectral density plots, we find that the mean signal strength in the expected transition zone is $\sim 10^{-20}$, while the effective noise due to numerical round-off errors is $\sim 10^{-22}$. Consequently, we take the same values as in § 3.2. We note that ζ is weakly dependent on the value of b, so that reducing b by a factor of 5 (as might naively be expected from increasing the scale height by the same factor) results in a negligible reduction of the threshold value to $\zeta = 1.15$. The plots of ζ for all models are shown in Figure 5.

Because the transition between confusion-limited signal to individually resolvable sources occurs over a spread of frequencies,

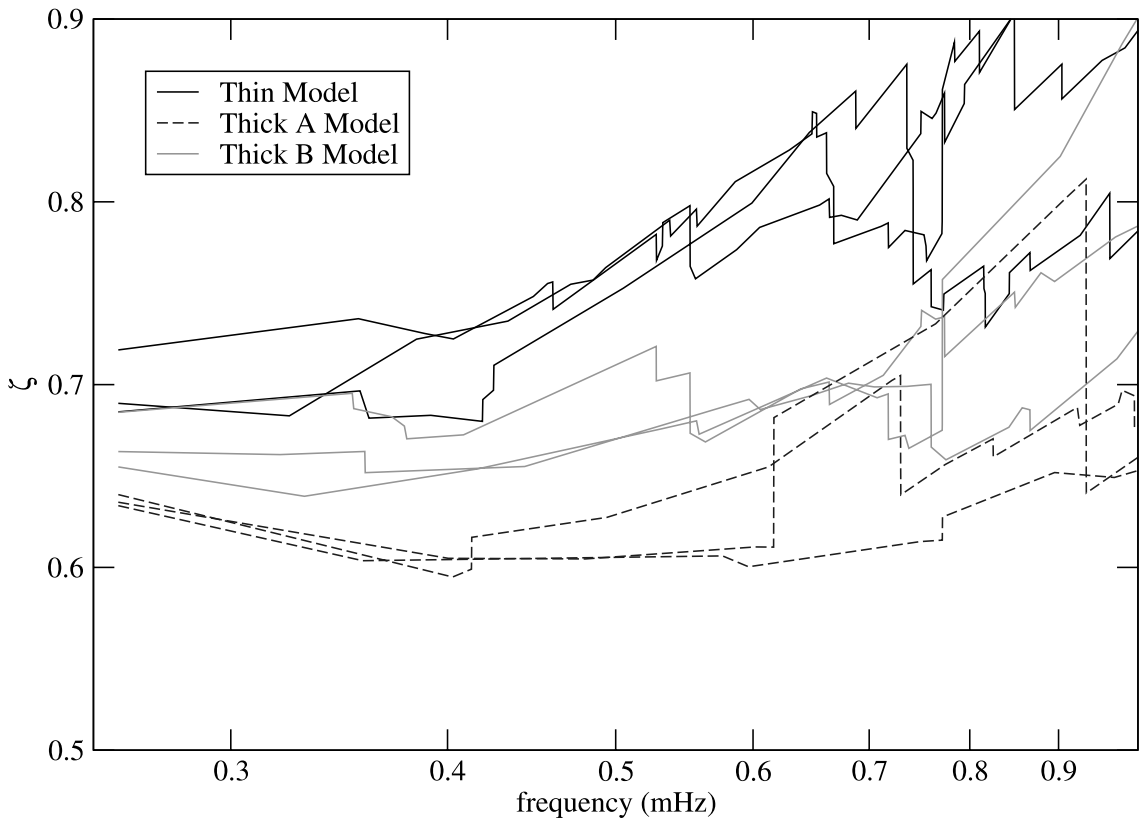

FIG. 7.—Plot of ζ as a function of frequency (in mHz) for the three realizations of each model. Note that the Thin model (*black line*) is above the Thick B model (*light gray line*), which is above Thick A (*dashed dark gray line*).

ζ can fluctuate about 1.2 over a range of frequencies. Furthermore, regions where random clustering of particularly loud signals can stand well above the confusion-limited noise will also produce values of ζ above 1.2. The range of frequencies through which ζ transitions past 1.2 are given for each model in Table 3. It is clear from Figure 5 that using a larger scale height for the Galaxy while maintaining the local space density of binaries results in a higher transition frequency, as would be expected from simply increasing the total number of binaries in the Galaxy. Also, we note that there is no significant difference in the value of f_t between the Thin and Thick B models. Again, this is not unexpected since all of these models contain the same number of binaries. We show in Figure 6 the appearance of the spectrum for the Thin model around 2.1 mHz to illustrate the separation of signals at this point. There are 76 binaries shown in Figure 6.

At the low-frequency end of Figure 5, there is an interesting distinction between all three models. Below about 1 mHz, the Thin model has a higher value of ζ than either Thick model, and the Thick A model has a lower value of ζ than the other two models. This detail is shown in Figure 7. It is understandable that the Thick A realizations should give a ζ below the Thin and Thick B models. The much larger total number of binaries in the Thick A models will produce a stronger confusion-limited signal from the thousands of binaries per frequency bin expected in the low-frequency end of the spectrum. Consequently, we would expect an overall smaller S/N for the bright signals that stand out above the background. This in turn will produce a smaller value of ζ due to the reduced value of b.

The explanation for the differences between the Thin and Thick B models is a little more subtle. First, we note that the background confusion-limited signal should be similar for both models, since they both have the same value of N (and therefore the same number of binaries per frequency bin). Furthermore, we used the same three random seeds to generate the three realizations of the Thin model as we used to generate the three realizations of the Thick B model, so the number density of binaries in frequency space cannot differ between the two models. Therefore, the differences in ζ between these two models cannot arise from different values of a. However, since the Thick B models have a larger scale height, the local space density is reduced by the ratio of scale heights. This, in turn, means that the average distance to the nearby binaries is larger in the Thick B models than the Thin models. Again, this will result in an overall lowering of the S/N of the bright signals compared with the Thin models, producing a smaller value of ζ in the Thick B models.

5. CONCLUSIONS

The canonical curve that is used to represent the Galactic white dwarf binary confusion-limited signal in descriptions of *LISA*'s sensitivity is based on a de facto local space density calibration of the total number of binaries in the Galaxy. The spatial distribution model that was used has a scale height of 90 pc (Hils et al. 1990). More recent models of the Galactic white dwarf binary population use a spatial distribution model with a scale height of 200 pc (Nelemans et al. 2001a, 2001b). Current estimates for the vertical scale height for white dwarfs in the disk are somewhat thicker, with scale heights between 240 and 500 pc (Nelson et al. 2002). The consequences of using an increased scale height in models of the Galactic white dwarf binary contribution to the *LISA* sensitivity curve differ depending on whether one calibrates the total number of binaries using global properties (such as inferred star formation history) or local properties (such as local space density). We have generated three models of the Galactic white dwarf binary population and calculated the expected *LISA* data stream from three realizations of each of these models. In order to analyze the expected transition frequency of the signal as it goes from confusion-limited to individually resolvable, we have introduced an estimator, ζ.

If the total number of binaries (N) in a Galactic binary simulation is calibrated by using the local space density, then an increase in the scale height of the spatial distribution model will result in a linear increase in the total number of binaries. In this case, the resulting change to the expected confusion curve is what one would expect from simply increasing the number of binaries. The transition frequency increases, and the overall level of the confusion-limited signal at low frequencies is increased. Since the local space density is used to calibrate N, the number of nearby low-frequency sources is unchanged by going to a larger scale height. The result of this is that fewer of these nearby sources will stand out above the low-frequency confusion-limited signal. Consequently, successfully extracting these bright sources will have less of an effect on the low-frequency confusion-limited signal than might be assumed from using a thin disk model, such as that found in Timpano et al. (2006).

If the total number of binaries is fixed by a global calibration method, the resulting effect of changing the scale height is considerably more subtle. Since the value of N is independent of the scale height, the expected transition frequency will not change. This is borne out by our analysis with the ζ estimator. In addition, the overall level of the low-frequency confusion-limited signal will change only negligibly due to the slight increase in the average distance to distant binaries. However, there can still be an effect on the low-frequency confusion-limited signal. With a fixed N, the local space density depends inversely on the scale height, so a larger scale height yields fewer expected nearby bright sources. Furthermore, the average distance to these nearby sources will increase for models with greater scale height. The net result is that fewer bright sources will be extractable from the low-frequency confusion-limited signal.

We would like to thank the anonymous referee for insightful comments that have helped us achieve a clearer picture of the effect of scale height on the confusion limit. We would like to acknowledge the support of the Aspen Center for Physics and the Center for Gravitational Wave Physics, which is funded by the National Science Foundation under the cooperative agreement PHY 01-14375. M. J. B. also acknowledges the support of NASA APRA grant NNG04GD52G. Work at the Aspen Center was supported by NASA Award Number NNG05G106G.

REFERENCES

Allen, C. W. 1973, Astrophysical Quantities (3rd ed.; London: Athlone)
Barack, L., & Cutler, C. 2004a, Phys. Rev. D, 69, 082005
———. 2004b, Phys. Rev. D, 70, 122002
Benacquista, M. J., DeGoes, J., & Lunder, D. 2004, Classical Quantum Gravity, 21, 509
Bender, P., & Hils, D. 1997, Classical Quantum Gravity, 14, 1439
Cornish, N., & Larson, S. 2003a, Phys. Rev. D, 67, 103001
———. 2003b, Classical Quantum Gravity, 20, 163
Cutler, C. 1998, Phys. Rev. D, 57, 7089
Edlund, J. A., Tinto, M., Krolak, A., & Nelemans, G. 2005, Phys. Rev. D, 71, 122003
Eggen, O. J., Lynden-Bell, D., & Sandage, A. R. 1962, ApJ, 136, 748

Evans, C., Iben, I., & Smarr, L. 1987, ApJ, 323, 129
Gilmore, G., & Reid, N. 1983, MNRAS, 202, 1025
Hils, D., & Bender, P. 1997, Classical Quantum Gravity, 14, 1439
Hils, D., Bender, P. L., & Webbink, R. F. 1990, ApJ, 360, 75
Kent, S. M., Dame, T. M., & Fazio, G. 1991, ApJ, 378, 131
Knox, R., Hawkins, M. R. S., & Hambly, N. C. 1999, MNRAS, 306, 736
Kuijken, K., & Gilmore, G. 1989, MNRAS, 239, 651
Marsakov, V. A., & Shevelev, Yu. G. 1995, Astron. Rep., 39, 559
Mihalas, D., & Binney, J. 1981 Galactic Astronomy: Structure and Kinematics (San Francisco: Freeman)
Miller, G. E., & Scalo, J. M. 1979, ApJS, 41, 513
Nelemans, G. 2003, Classical Quantum Gravity, 20, 81
Nelemans, G., Yungelson, L. R., & Portegies Zwart, S. F. 2001a, A&A, 375, 890
———. 2004, MNRAS, 349, 181
Nelemans, G., Yungelson, L. R., Portegies Zwart, S. F., & Verbunt, F. 2001b, A&A, 365, 491
Nelson, C. A., Cook, K. H., Axelrod, T. S., Mould, J. R., & Alcock, C. 2002, ApJ, 573, 644
Ojha, D. K., Bienaymé, O., Robin, A. C., Crézé, M., & Mohan, V. 1996, A&A, 311, 456
Postnov, K., & Prokhorov, M. 1998, ApJ, 494, 674
Reed, C. 2000, BAAS, 32, 710
Rubbo, L. J., Cornish, N. J., & Poujade, O. 2004, Phys. Rev. D, 69, 082003
Schröder, K.-P., & Pagel, B. E. J. 2003, MNRAS, 343, 1231
Siebert, A., Bienaymé, O., & Soubiran, C. 2003, A&A, 399, 531
Steinmetz, M., & Navarro, J. F. 2002, NewA, 7, 155
Takahashi, R., & Seto, N. 2002, ApJ, 575, 1030
Timpano, S., Rubbo, L., & Cornish, N. 2006, Phys. Rev. D, in press (gr-qc/0504071)
Umstätter, R., Christensen, N., Hendry, M., Meyer, R., Simha, V., Veitch, J., Vigeland, S., & Woan, G. 2005, Classical Quantum Gravity, 22, 901
———. 2005, Phys. Rev. D, 72, 022001
Vecchio, A., & Wickham, D. L. 2004, Phys. Rev. D, 70, 082002
Webbink, R. F. 1984, ApJ, 277, 355
Wielen, R. 1977, A&A, 60, 263